Impact of quadric surface carrier on gas flow radial dispersion pattern in a vehicle catalytic converter

B. Ding

School of Traffic, Northeast Forestry University, Harbin, Heilongjiang, China

In a conventional vehicle catalytic converter with flat-end carrier and common diffusion header, most of engine exhaust passes through a small-radius tubular part of the centre of the honeycomb carrier where the catalyst is rapidly deteriorated with high load and the honeycomb is easily fragmented on thermal stress. To improve the radial distribution of the exhaust gas by optimizing the structure of the converter is valuable in theory and practice for enhancing the conversion, service life, and reducing the cost. In this study, numerical simulation and experiment verification of the gas flow in an automotive catalyst converter with several quadric surface-shaped honeycomb carriers were performed based on ANSYS-CFD code and test, and the influence of the carrier fore-end types matching of diffusion headers on flow radial uniformity was studied. The effects show that cone-headed and sphere-headed honeycomb carriers improved the flow radial distribution especially in a cone-headed honeycomb carrier matching an enhanced diffusion header (EDH), thus the uniformity evaluation index can be increased by 29.4%–33.9%. The cone apex angle should be controlled between 60° and 90° so as to get comprehensive advantages of better flow distributional uniformity along desired radial reliability and small size of converter.

Key words: Vehicle catalyst converter, Quadric surface honeycomb carrier, Diffusion header, Numerical simulation, Gas flow radial dispersion, Uniformity evaluation index.

INTRODUCTION

Catalyst converters are currently widely used as the most effective way to reduce the harmful exhaust from the vehicle engine, and are extended to the field of large marine and mining engines [1-3]. With research in depth, the gas flow radial distribution, which has great influence on conversion efficiency and service life, has become one of the primary valuations for designing automotive catalyst converters [4-5]. Normally, the structure of a conventional diffuser matching with a planar fore-end honeycomb carrier hardly permits satisfying diffusion, so that the gas flow radial distribution is clearly not uniform, which leads to low conversion efficiency, faster local deterioration, higher radial thermal stress and shorter service life of the catalyst converter [6]. This problem exists not only in a under-body catalytic converter but also in others such as exhaust manifold converter, close coupled converter, supercharger coupled converter, which is caused by internal structure of the converter [7-8]. To improve the internal gas diametral distribution, a number of unconventional fore-end shaped honeycomb carriers including quadric surface and diffusions were designed. The flow fields of these new types of catalyst converters were simulated based on ANSYS-CFD. In the experiment, the effects of gas flow radial distribution on some fore-end shaped honeycomb

carriers coupled with different types of diffusers were discussed, and the internal structure of the catalyst converter was optimized.

SIMULATION OF GAS FLOW PATTERN IN THE CONVERTER

Considering the structure of the honeycomb ceramic carrier catalyst and the flow condition of the engine exhaust, the numerical simulation adopted the mathematical model based on Newton fluid dynamics theory.

Gas flow control equation

For a steady gas flow, the mass and momentum conservation equations are as follows [9]:

$$\frac{\partial}{\partial x_j}(\rho V_j) = 0 \tag{1}$$

$$\frac{\partial}{\partial x_j}(\rho V_j V_i + \tau_{ij}) = -\frac{\partial p}{\partial x_i} + s_i \tag{2}$$

where: V_i, V_j - velocity in the direction of i, j; x_i, x_j - displacement in the direction of i, j; p - fluid pressure; ρ - fluid density; s_i - source referring to the resistance of the honeycomb carrier; τ_{ij} - viscous stress for Newtonian fluids;

$$\tau_{ij} = 2\mu s_{ij} - \frac{2}{3}\mu\delta_{ij}\frac{\partial V_k}{\partial x_k} + \tau_{ij}^{(T)} \tag{3}$$

where: μ - viscosity coefficient; δ_{ij} - Kroneker function; $\tau_{ij}^{(T)}$ - Reynolds stress tensor due to

turbulent pulsation, $\tau_{ij}^{(T)} = -\overline{\rho V_i' V_j'}$; s_{ij} - strain rate tensor given with the following equation:

$$s_{ij} = \frac{1}{2}(\frac{\partial V_i}{\partial x_j} + \frac{\partial V_j}{\partial x_i}) \qquad (4)$$

Turbulence model

Reynolds stress can be calculated with a typical k-ε model to self-contain the above gas flow control equation:

$$\tau_{ij}^{(T)} = 2\mu_T s_{ij} - \frac{2}{3}\rho k \delta_{ij} \qquad (5)$$

where: μ_T refers to the turbulence viscosity coefficient given with:

$$\mu_T = \rho C_\mu \frac{k^2}{\varepsilon} \qquad (6)$$

k—turbulent kinetic energy, $k = \frac{1}{2}\overline{V_i' V_i'}$, meeting the following equation:

$$\rho\frac{\partial k}{\partial t} + \rho V_j \frac{\partial k}{\partial x_j} = \frac{\partial}{\partial x_j}[(\mu + \frac{\mu_T}{\sigma_k})\frac{\partial k}{\partial x_j}] + S_k \qquad (7)$$

where: $S_k = P_k - D_k$, $P_k = \tau_{ij}^{(T)}\frac{\partial V_i}{\partial x_j}$, is the originative term, $D_k = \rho\varepsilon$, is the dissipative term; ε—turbulent dissipation rate, $\varepsilon = \upsilon\overline{\frac{\partial V_i'}{\partial x_k}\frac{\partial V_i'}{\partial x_k}}$, meeting the following equation:

$$\rho\frac{\partial \varepsilon}{\partial t} + \rho V_j \frac{\partial \varepsilon}{\partial x_j} = \frac{\partial}{\partial x_j}[(\mu + \frac{\mu_T}{\sigma_\varepsilon})\frac{\partial \varepsilon}{\partial x_j}] + S_\varepsilon \qquad (8)$$

where: $S_\varepsilon = P_\varepsilon - D_\varepsilon$, $P_\varepsilon = C_{\varepsilon 1}\frac{\varepsilon}{k}\tau_{ij}^{(T)}\frac{\partial V_i}{\partial x_j}$, is the originative term, $D_\varepsilon = C_{\varepsilon 2}\rho\frac{\varepsilon^2}{k}$, is the dissipative term.

Gas flow model in a honeycomb carrier

As a kind of porous medium, the honeycomb ceramic carrier is composed of many same-sized tiny rectangular tubes parallel with the axis of the converter. It can be simulated by the equivalent continuous method [10]. If the resistance is very high, the convection term and the diffusion term will be neglected. Then the momentum equation can be simplified as:

$$\frac{\partial p}{\partial x_i} = -K_i V_i \qquad (9)$$

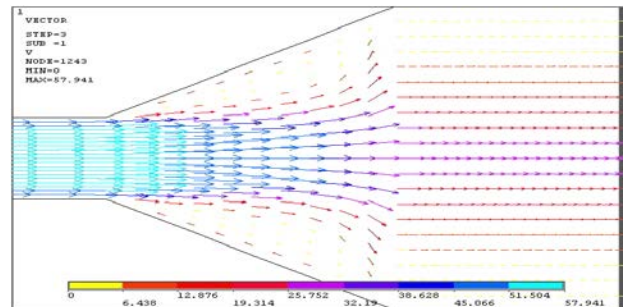$$K_i = \alpha_i|\vec{V}| + \beta_i \qquad (10)$$

where: K_i—permeability, which is proportional to the velocity at the relevant position; α_i, β_i—empirical constants, which take the value of 1×10^5

both in the radial and circumferential directions of the honeycomb carrier, in the case of considering the gas flow just along the axial direction and no mass exchange in the radial and circumferential directions.

Simulative boundary conditions

With the above model, simulation was based on the module FLOTRAN CFD. Normally, being an axisymmetric automotive analyst converter, the gas flow is treated as a planar flow passing by the symmetry axis. Numerous parallel tubes are distributed in a unit cross-sectional area of the honeycomb carrier and the equivalent diameter of the tubes is very small. Thus, in the range of displacement of automotive engine, the gas flow in the carrier can be regarded as a steady laminar flow. During the simulation, the axial velocity of the gas flow through the intake of the converter was assumed to be uniform in diameter, and the range adopted was 17–53 m/s, circumferential and radial velocity was zero. Meanwhile, the gas flow inlet pressure was made 1MPa, inlet temperature was made 293.0K. At the exit side of the converter, a well-developed laminar flow was made, the pressure could be assumed as atmospheric pressure, and the boundary was no-slip.

One of the gas flow field diagrams simulated inside the catalytic converter is shown in Fig. 1.

Conventional plane fore-end carrier, 30º semi-angle diffuser
Fig. 1. Gas flow field diagram simulated inside the converter

EXPERIMENTS

In order to verify the reliability of the flow field numerical model, a testing system was set up and the velocity of the gas flow in the catalyst converter was measured. One of the test devices is schematically shown in Fig. 2. Using air as the gas flow supply and cordierite honeycomb carrier as the uncovered fore-end shaped carrier, the radial distribution of the axial velocity of the gas through the carrier was tested with Y-style Pitot tube on the steady flow test bed.
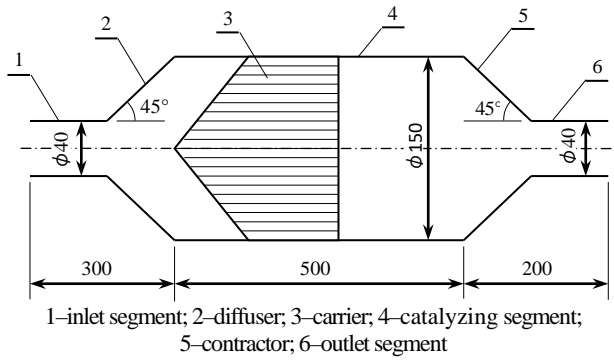
1–inlet segment; 2–diffuser; 3–carrier; 4–catalyzing segment;
5–contractor; 6–outlet segment

Fig. 2. Structure of the experimental converter

Some of the results are shown in Fig. 3, indicating the comparison between the test and calculated results. With a series of experiments, the test data were well able to match the calculated results, which was satisfying for discussing the character of gas flow in different types of converter and analyzing the diametral distribution of the gas flow.
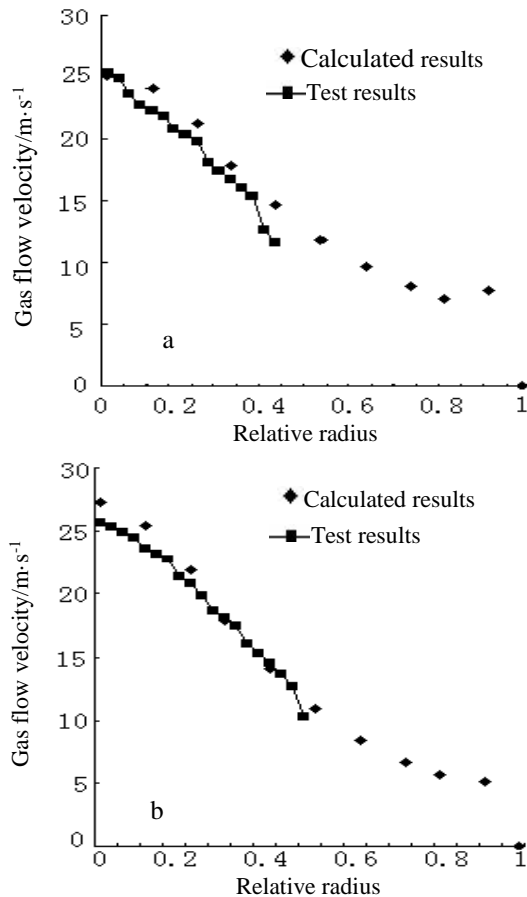

Fig. 3. Testing results and calculating results of gas flow velocity. a) 90º Fore-end shaped cone carrier, 30º semi-angle diffuser; b) 120º Fore-end shaped cone carrier, 30º semi-angle diffuser

OPTIMIZING THE STRUCTURE

Uniformity evaluation index of gas flow radial distribution

Neglecting the on-way resistance, the difference between the diameter of the inlet segment and the catalyzing segment is the cause of the non-uniform gas flow radial distribution in the catalyst converter. Considering the radial difference, in order to test the effects on different fore-end shaped carriers matching with different diffusers under the same condition, the ratio $\gamma_{0.3}$ of mean gas flow velocity in the whole carrier cross section to mean flow velocity in the cross-sectional area of relative radius of 0.3 around the converter axes was defined as the index for evaluating the uniformity of gas flow radial distribution:

$$\gamma_{0.3} = \frac{\bar{v}}{\overline{v_{0.3}}} \tag{11}$$

where: $\bar{v}$ - mean flow velocity of the gas flow at the whole carrier cross section along the converter axes, m/s; $\overline{v_{0.3}}$ - mean flow velocity in the cross-sectional area of a relative radius of 0.3, m/s.

The definition is related to the diameter ratio of the catalyzing segment to the inlet segment. It satisfies the conformity of the experimental conditions and is able to testify the internal gas flow distributional uniformity in diameter. It also can be extended to automotive analyst converters with different inlet segments and catalyzing segment diameters based on its essence.

Fore-end shape of the carrier

With the maintained numerical model and boundary conditions, the internal gas flow field with different fore-end shaped carriers was simulated. The radial distribution curves of the axial gas flow velocity through the cross section of the carriers are shown in Fig. 4. In Table 1, the flow uniformity index is presented.
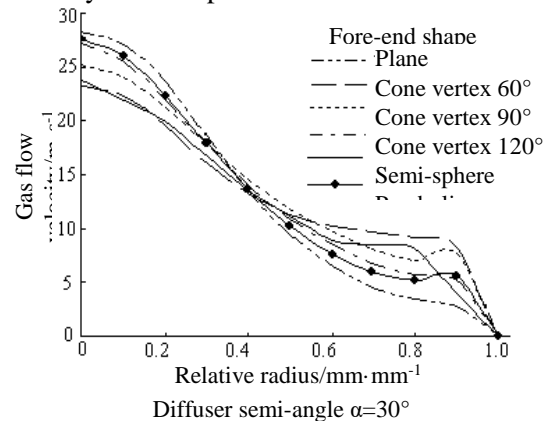

Diffuser semi-angle α=30°

Fig. 4. Radial distribution of gas flow velocity with different fore-end shaped carriers

Table 1 Flow uniformity index with different fore-end shaped carriers[1]

Forer-end shape of carrier		$\gamma_{0.3}$
Conventional plane		0.5645
Parabolic	Vertex 120°	0.6318
Sphere		0.6636
Cone	Vertex 120°	0.6504
	Vertex 90°	0.6944
	Vertex 60°	0.7056

Note: [1]Catalyst converter diffuser semi-angle α=30°

When using the fore-end shaped cone carrier, the gas flow radial distribution uniformity was clearly improved and the gas flow uniformity increased with the decrease in the vertex angle. With the same vertex angle, the uniformity index of the parabolic fore-end was smaller than that of the cone-shaped fore-end. Consequently, shaped fore-end structure is in a way working as a baffler. The smaller the vertex angle, the better are the effects of gas flow radial diffusion. However, undersized vertex angle will unbalance the honeycomb carrier, which is unfavorable for fixing and sealing carrier and will increase the volume of the catalyst converter. Considering the technologic processing of production, it is inadvisable to make the vertex angle over 60°.

Diffuser structure matching with carrier

Effects of different diffusers matching with different honeycomb carriers on the gas flow radial distribution were simulated, where the diffusers included four types such as 30°, 45°, 60°-semi-angle and enhanced diffusion header (EDH); the honeycomb carriers included five types such as planar fore-end, 90° vertex angle fore-end, 120° vertex angle fore-end, semisphere fore-end and parabolic fore-end. In some cases of different inlet gas flow velocity, Fig. 5 indicates the difference of gas flow radial distribution between 30°-semi-angle diffuser matching with a conventional planar fore-end carrier and EDH matching with 90° vertex angle fore-end carrier. Detailed uniformity indices with different matching are shown in Table 2.

From the simulation results it can be seen that matching with different diffusers, planar and parabolic fore-end carriers normally led to poorer diffusion. Matching with a 60° or 45° semi-angle diffuser led to the lowest uniformity index, where the parabolic fore-end shape made a better improvement than planar fore-end when the diffuser semi angle was less than 45°. The reverse was observed when the diffuser semi-angle was over 45°. Sphere- and cone-shaped carriers both improved the radial diffusion, and the uniformity index $\gamma_{0.3}$ considerably increased. EDH matching with 90° cone carrier led to the best improvement of distribution, and the uniformity index increased by 29.4%–33.9% compared to the conventional structure.
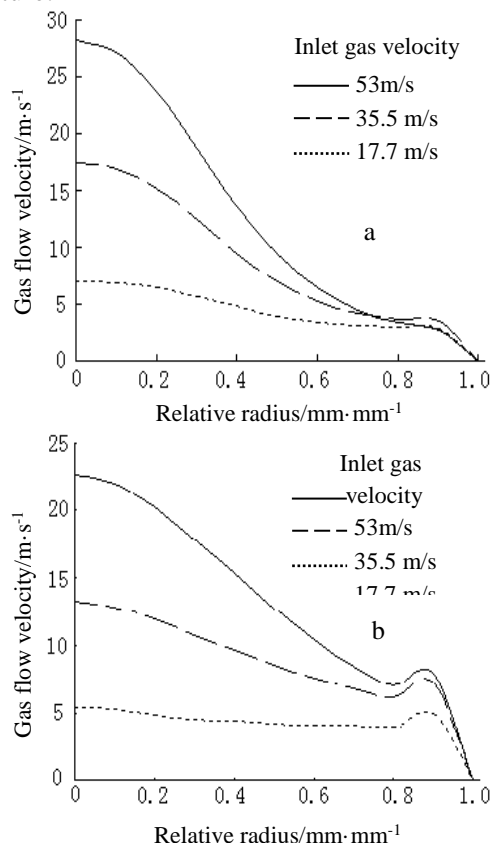

Fig. 5. Gas flow radial distribution with two different matchings; a) 30° semi-angle diffuser, conventional fore-end shaped planar carrier; b) EDH, 90° fore-end shaped cone carrier

Table 2 Radial diffusion with different matchings[1]

Diffuser	Fore-end shape of carrier	$\gamma_{0.3}$	Diffuser	Fore-end shape of carrier	$\gamma_{0.3}$
30° Semi-angle	Plane	0.5645	60° Semi-angle	Plane	0.5225
	Parabolic	0.6318		Parabolic	0.5201
	Sphere	0.6636		Sphere	0.5230
	Vertex 120°	0.6504		Vertex 120°	0.5235
	Vertex 90°	0.6944		Vertex 90°	0.5464
45° Semi-angle	Plane	0.5407	EDH	Plane	0.6576
	Parabolic	0.5522		Parabolic	0.6528
	Sphere	0.5968		Sphere	0.6854
	Vertex 120°	0.5921		Vertex 120°	0.6646
	Vertex 90°	0.6210		Vertex 90°	0.6998

Note: [1]Inlet gas flow velocity: 53m/s

CONCLUSIONS

(1) A new uniformity index was defined more distinctly and logically than traditionally to evaluate gas flow radial distribution in automobile catalytic converters.

(2) Compared to the fore-end shaped planar carrier, the cone or sphere carrier lead to better gas flow radial distribution in the automotive catalyst converter. The improvement is prominent when using the cone carrier, especially when the vertex is under 90°. In the simulation and experiment, smaller vertex is able to increase the uniformity index. Comprehensively considering the technologic processing of production, reliability and tight structure, a vertex angle within the range of 60°-90° was suggested.

(3) Fore-end shaped cone carrier matching with EDH makes the best improvement of the gas flow diametral distribution. Especially when a 90° vertex carrier matches with EDH, the uniformity index can be increased by 29.4%–33.9%.

REFERENCES

1. A. Mukherjee, K. Roy, J. Bagchi, K Mondal, *Journal for Research*, **2**, 29 (2016).
2. D. Bernečić, R. Radonja, *Scientific Journal of Maritime Research*, **25**, 15 (2011).
3. D.H. Wang, M.Q. Zou, *Coal Mine Machinery*, **37**, 55 (2016).
4. B. Liu, Y. Liang, L.Y. Zhou, J. Wang, *Journal of Hunan University (Natural Sciences)*, **31**, 17 (2004).
5. S.P. Harshil, J.P. Dipak, *International Journal for Scientific Research & Development*, **3**, 74 (2015).
6. S.J. Jeong, W.S. Kim, *Chemical Engineering Communications*, **189**, 1314 (2002).
7. B.Q. Ding, M.Y. Li, *Vehicle Engine*, **3**, 20 (2011).
8. C.P. Om Ariara Guhan, G. Arthanareeswaran, K.N. Varadarajan, S. Krishnan, *Journal of Computational Design and Engineering*, **3**, 198 (2016).
9. D.Q. Mei, Z.X. Liu, Y. Miao, Sh. Zhang, *Vehicle Engine*, **3**, 10 (2013).
10. X.L. Chen, W.G. Zhang, Z. Huang, *Journal of Shanghai Jiaotong University*, **38**, 1205 (2004)